Effect of Sn Nanoparticle Additions on Thermal Properties of Sn-Ag-Cu Lead-free Solder Paste

Evan Wernicki and Zhiyong Gu*

Department of Chemical Engineering University of Massachusetts Lowell Lowell, MA 01854, U.S.

* Contact Information:

Department of Chemical Engineering University of Massachusetts Lowell One University Ave Lowell, MA 01854, United States

Phone: (1) 978-934-3540

 $Email: Zhiyong_Gu@uml.edu$

Abstract

Lead-free nanocomposite solder pastes were prepared with Sn-3Ag-0.5Cu (SAC 305)

microsolders, 1-5 wt% Sn nanoparticles, and a flux. The nanocomposite pastes were studied

using differential scanning calorimetry (DSC) to understand their thermal properties and the

interactions between the different sized powders. DSC measurements showed two distinct

endothermic peaks in all nanocomposite pastes with Sn nanoparticle additions, with one peak

attributing to the melting of SAC micropowders and another peak to the melting of Sn

nanoparticles. With the increased amount of Sn nanoparticle additions, the SAC material showed

little change in its melting temperatures due to its large mass fraction. Multi-cycle DSC

measurements of the nanocomposite solder pastes showed additional endothermic peaks,

suggesting that the SAC 305 microsolder powders and pure Sn nanoparticles may have

interacted with each other to form additional alloys. Changes in enthalpy of melting from DSC

measurements were also used to analyze the melting characteristics of the nanocomposite pastes.

Additionally, thermogravimetric analysis (TGA) measurements showed that more weight was

retained for the nanocomposite solder pastes with increasing Sn nanoparticle additions,

compared to the baseline SAC solder paste.

KEYWORDS:

Solder paste; Sn-Ag-Cu (SAC); nanoparticles; nanocomposite; DSC

1. Introduction

Solders are important materials due to their widespread use as interconnect materials in electronics assembly and packaging applications [1-3]. The ease of use for attaching and rework, relatively low cost, and wide availability of material property data make solder a good choice for many interconnect applications [4]. The solder materials also provide good electrical, mechanical and thermal properties. The creation of an inter-metallic compound (IMC) at the solder/substrate interface forms the metallurgical bond between the solder and substrate materials [5]. Homogenously dispersing solder micropowders within a flux matrix, known as solder pastes, allow for screen-printing to selectively deposit it on electrically conductive pads on both large and small manufacturing scales. It is important that the solder paste be able to fully melt and form a strong metallurgical bond to the pad surface. During reflow, the solder powders melt, coalesce and wet the substrate to form a metallurgical joint. The microstructure and its mechanical properties are heavily dependent on solder composition, bond pad material, reflow conditions and aging conditions [6-13]. For more reliable interconnections in surface mount technology (SMT) processes, it is desired to have materials with stronger mechanical properties.

Tin-silver (Sn-Ag) hypereutectic alloys have fine microstructures with uniform dispersions of stable Ag₃Sn IMC precipitates surrounding β-Sn dendrites and exhibit better mechanical properties than Pb-Sn solder alloys [3, 14, 15]. Small additions of copper (Cu) to form a ternary Sn-Ag-Cu (SAC) alloy were observed to improve wetting and mechanical properties of the solder [16] by introducing an additional strengthening phase, Cu₆Sn₅ [17, 18]. The Sn-Ag-based alloys have been the favored Pb-free choices because of their good mechanical properties, acceptable wetting properties, as well as suitable melting points [1, 18-21].

Recently, nanocomposite solder pastes have been extensively studied by combining microsolders with nanomaterials of pure metals [22-24], ceramics [25-27], intermetallic compounds [28], organic materials [29] and alloy nanoparticles [30]. Changes in mechanical properties [30] and IMC growth [26, 27] have been reported when compared with their respective microsolder materials. Lin et al. observed an effect on the supercooling, up to 5 °C, of a paste mixture when adding Cu nanoparticles due to the alloying of Cu with Sn and suggested a local ternary Sn-Ag-Cu alloy was formed [31]. Bukat et al. investigated Ag nanoparticles in a Sn-Ag-Cu paste system and observed star-like Ag₃Sn when adding 4 wt% Ag nanoparticles due to alloying with the Sn from the Sn-Ag-Cu solder [5]. Lead-free nanosolder pastes have also been studied by combining Sn [32, 33], Sn-Ag [34, 35], Sn-Ag-Cu [36] or Sn-Co-Cu [37] nanoparticles with a flux in an attempt to take advantage of melting temperature depressions that can occur in nanomaterials. Issues such as low particle loading, surface oxidation and incomplete solder coalescence have limited the application of nanosolder pastes unless excess flux was used [33], or capping layers were left on the surfaces of the nanoparticles [33, 35]. However, to the best of our knowledge, there are no detailed reports investigating the melting behavior and thermal properties of Pb-free solder pastes when nanomaterials having similar melting temperatures or compositions are added into the solder paste.

In this work, nanocomposite solder pastes were prepared by homogenously mixing Sn-3Ag-0.5Cu (SAC 305) microsolders, Sn nanoparticles (1-5 wt%), and a flux. The thermal properties of the nanocomposite pastes were investigated via differential scanning calorimetry (DSC) to observe the melting behavior of the SAC 305 microsolders and Sn nanoparticles when heated to above their respective melting temperatures. Multi-cycle DSC measurements were used to characterize the nanocomposite solder pastes after solder melting and coalescence to compare the

changes in melting temperature and enthalpy of melting. Additionally, thermogravimetric analysis (TGA) was used to investigate the effect of Sn nanoparticles on the decomposition behavior of the nanocomposite solder pastes.

2. Experimental

2.1 Materials & Chemicals

Sn nanoparticles (99.9%) used in preparing the nanocomposite solder pastes were purchased from US Research Nanomaterials, Inc. The flux material used was an Indium 8.9E paste flux provided by Indium Corporation (Clinton, NY). SAC 305 solder powders (type 4) were also provided by Indium Corporation.

2.2 Solder Size and Morphology

A JEOL JSM 7401F field-emission scanning electron microscope (FESEM) was used to observe and confirm the size and morphology of the Sn nanoparticles and SAC 305 type 4 microsolder powders. Energy dispersive x-ray spectroscopy (EDS) was used to confirm the purity and composition of the Sn nanoparticles and type 4 SAC powders.

2.3 Preparation of Solder Pastes

Nanocomposite solder pastes were prepared by homogenously dispersing micro and nanoparticle with the material using a Thinky AR-100 centrifugal mixer. All materials were weighed in a 12 mL mixing container and pastes were all prepared with a total solder loading of 82.5 wt%. The flux was weighed first followed by the appropriate amount of Sn nanoparticles and SAC 305 powders. Dependent upon the Sn nanoparticle addition amount in the paste, the powder weight was adjusted accordingly. The container was immediately sealed using the screw cap and placed in the mixer. The pastes were mixed for 3 minutes at 1600 rpm after balancing the mixer using

the adjustable weight. An Olympus CX-41 optical microscope equipped an Olympus DP71 digital camera was used to characterize mixing and powder dispersion after mixing.

2.4 DSC/TGA Measurements

Thermal measurements of the prepared nanocomposite pastes were performed using a TA Instruments Discovery Q1000 differential scanning calorimeter (DSC) at a scan rate of 10 K/min to analyze and identify melting and solidification. Cyclic procedures were used in DSC measurements to identify changes in melting as a result of the Sn nanoparticle additions. Hermetically sealed aluminum (Al) DSC pans were used for all samples tested. A TA Instruments Discovery TGA was used to measure the solder powder materials and nanocomposite solder pastes conducted with a scan rate of 10 K/min. Paste samples were placed on a hermetic Al DSC pan and placed on the 100 µL TGA pan. DSC spectra were analyzed using the TRIOS software (V. 4.2) by TA Instruments. The built-in analysis tools were used to calculate the onset temperatures of melting, peak melting temperatures, and normalized enthalpy of melting.

3. Results and Discussion

3.1 Characterization of SAC Micropowders and Sn Nanoparticles

Electron microscopy images of the SAC micropowders and Sn nanoparticles are shown in Figure 1. Figure 1A showed that the type 4 SAC 305 micropowders are spherical and uniform in size. A size analysis of the microsolders showed an average diameter of $28.4 \pm 4.7 \,\mu m$ and are within the established IPC criteria for type 4 solder powder classification (20 - $38\mu m$) [38]. The Sn nanoparticles in Figure 1B were also observed to be mostly spherical with an average diameter of $84 \pm 13.3 \, nm$. Figure 2 shows the energy dispersive x-ray spectroscopy (EDS) spectra for the

SAC 305 micropowders and Sn nanoparticles. It was observed that Sn, Ag and Cu were identified for the SAC 305 microsolders. For the Sn nanoparticles, only Sn was detected in the nanoparticles indicating no observable impurities. Silicon (Si) was used as the substrate for holding both samples for electron microscopy imaging and EDS analysis.

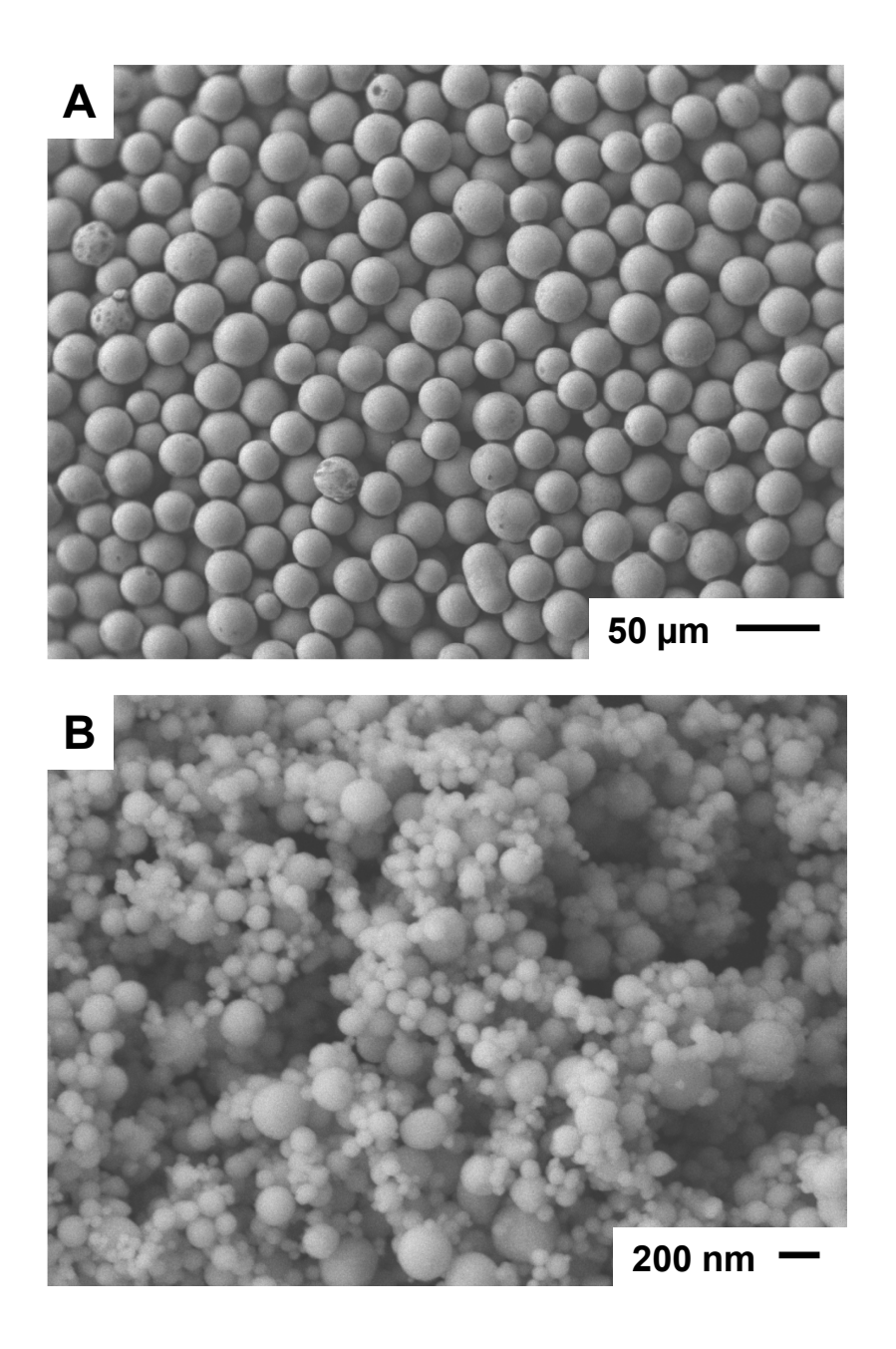


Fig. 1: SEM images of (A) SAC 305 Type 4 microsolders and (B) Sn nanoparticles used in preparing the nanocomposite solder pastes.

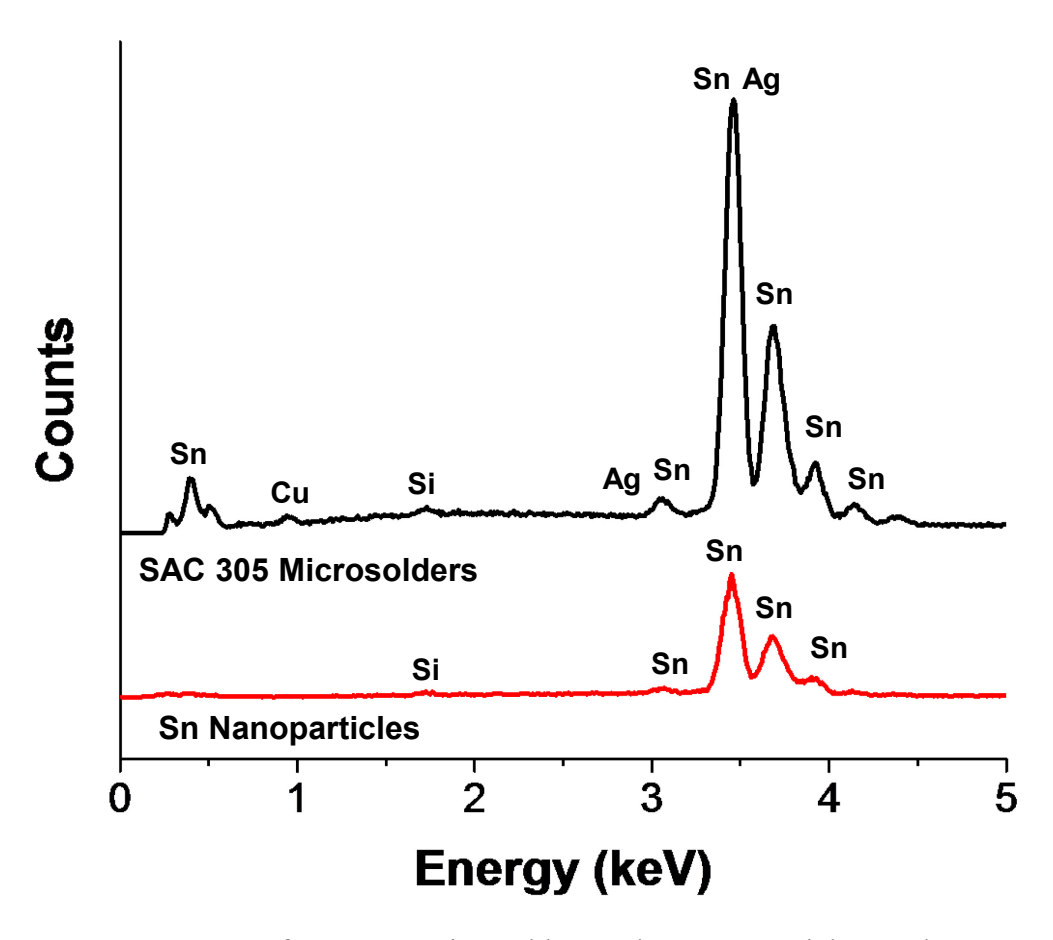


Fig. 2: EDS spectra of SAC 305 microsolders and Sn nanoparticles used to prepare the nanocomposite solder pastes.

3.2 DSC/TGA Measurements of SAC Micropowders and Sn Nanoparticles

The melting temperatures of the solder materials were measured by DSC, shown in Figure 3. The SAC 305 solder system has been widely studied and has been reported to have an onset melting temperature of 217 °C [17, 20, 39, 40]. In Figure 3A, the melting temperature range of the SAC 305 micropowders matched well with the reported values, with an onset temperature of 216.9 °C and a peak temperature of 219.5 °C. In comparison, bulk Sn has a melting temperature of 231.91 °C [41]. In Figure 3B, the Sn nanoparticles showed an onset melting temperature of 227.4 °C and a peak temperature of 232.3 °C, which is very close to the bulk Sn and no significant melting

temperature depression was observed. Jiang et al. reported a peak melting temperature of 231.8 $^{\circ}$ C for as-synthesized Sn nanoparticles with a diameter of 85 \pm 10 nm through DSC measurements [32], which is very close to the value measured in this study.

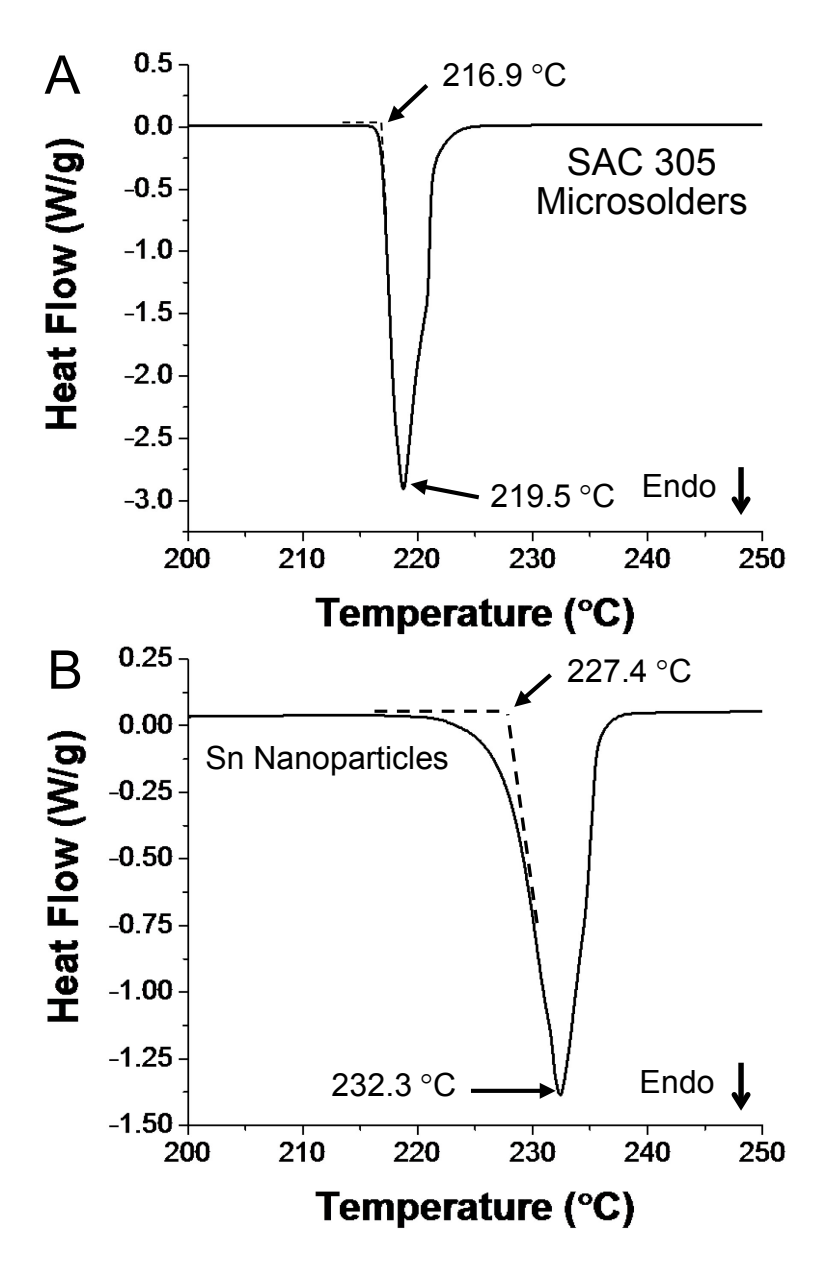


Fig. 3: DSC measurements of (A) SAC 305 microsolders and (B) Sn nanoparticles at a heating rate of 10 K/min.

TGA measurement of the SAC 305 microsolder material is shown in Figure 4, indicating a minimal change in weight during heating, about a maximum of 0.2 % more weight than its original mass when heated up to 500 °C. The slight increase in mass was most likely due to surface oxidation of the micropowders in the air atmosphere during heating. Sn nanoparticles were observed to decrease in weight when heated up to 180 °C. This initial weight loss could be from the decomposition of some impurities present on the surface of the Sn nanoparticles during manufacturing. Compared to the SAC 305 microsolders, significantly more weight gain was observed in the Sn nanoparticles after ~ 200 °C. Surface oxidation is likely the reason for the increased weight gain for Sn nanoparticles, coinciding with the much greater surface area to volume ratio of the nanoparticles compared to the micropowders and their more prone to oxidation in the atmosphere. Accounting for the initial weight loss, the Sn nanoparticles were measured to gain 17 times more weight than the SAC 305 powders during heating in TGA measurements, in the same temperature span from room temperature to ~ 500 °C.

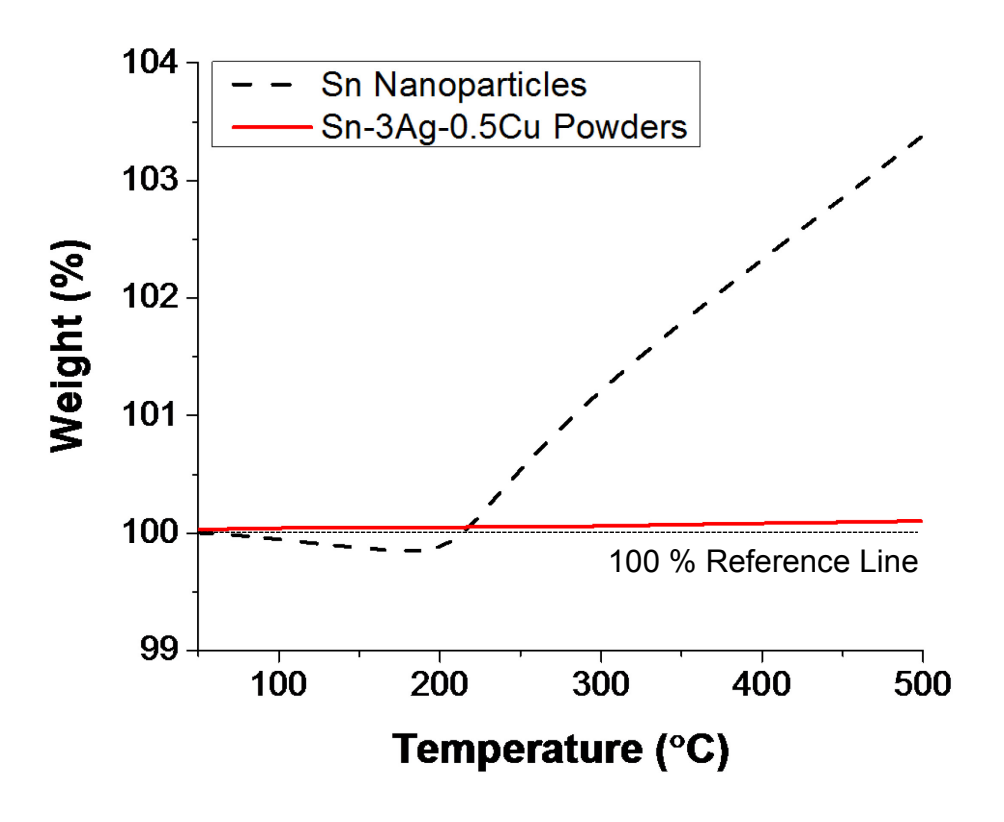


Fig. 4: TGA measurements of SAC 305 micropowders and Sn nanoparticles.

3.3 DSC Measurements of Nanocomposite Solder Pastes

Nanocomposite solder pastes were measured using DSC to observe the influence of the Sn nanoparticles on the thermal behavior of the pastes when heated above the melting temperature of both the micropowders and nanoparticles. The overall DSC spectra for pastes during the initial heating cycle are shown in Figure 5. In all pastes, a large endothermic peak was first observed with an onset melting around 217 °C (ranged from 217.2 to 217.4 °C) (See Table 1). In pastes containing Sn nanoparticles, a second endothermic peak was observed attributing to the melting of the Sn nanoparticles in the paste. The endothermic peak from Sn nanoparticle melting was observed to increase with greater Sn nanoparticle additions. The paste was mainly comprised of

SAC 305 micropowders, therefore the endothermic peak associated with SAC melting was greater than that of the Sn nanoparticles.

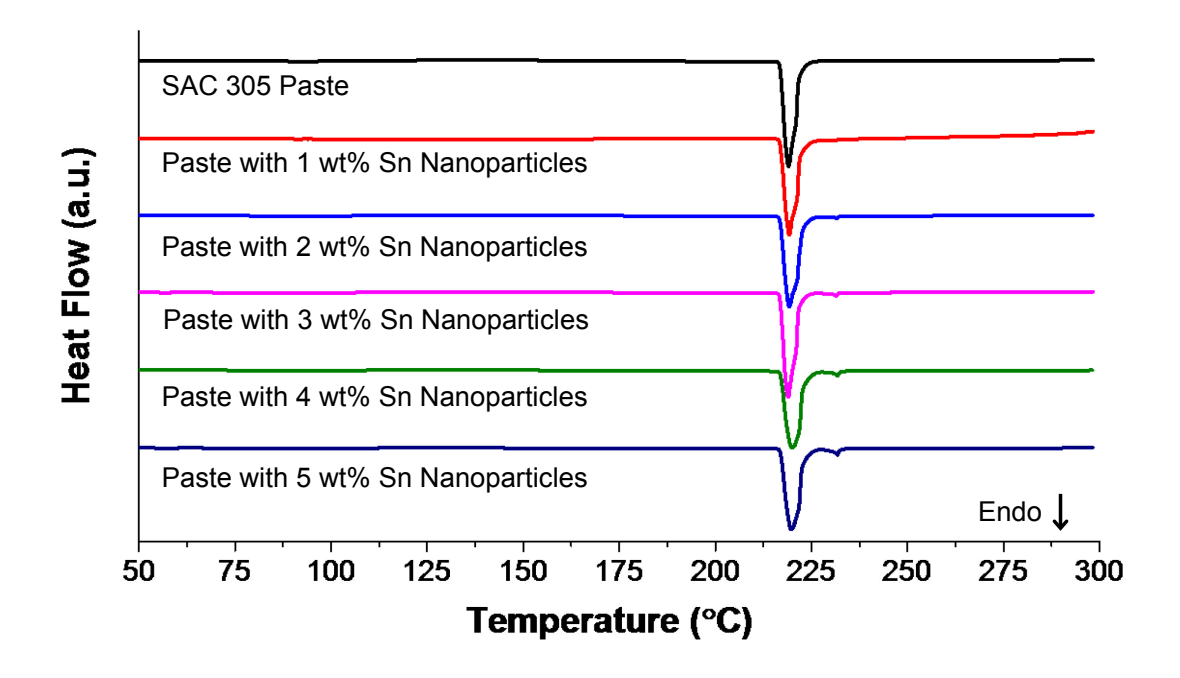


Fig. 5: DSC curves showing the initial heating and melting of the prepared solder pastes with Sn nanoparticle additions. All pastes were scanned at 10 K/min.

Figure 6A shows the endothermic peaks from the SAC 305 during the initial heating, in the temperature range from 215 °C to 225 °C. It was observed that the onset of SAC melting remained mostly unchanged when adding Sn nanoparticles. A small variation in peak melting temperature was observed with the additions of Sn nanoparticles, up to 3 wt%. Further increases in nanoparticle additions (up to 5 wt%) caused a slight increase in the peak melting temperatures (see Table 1).

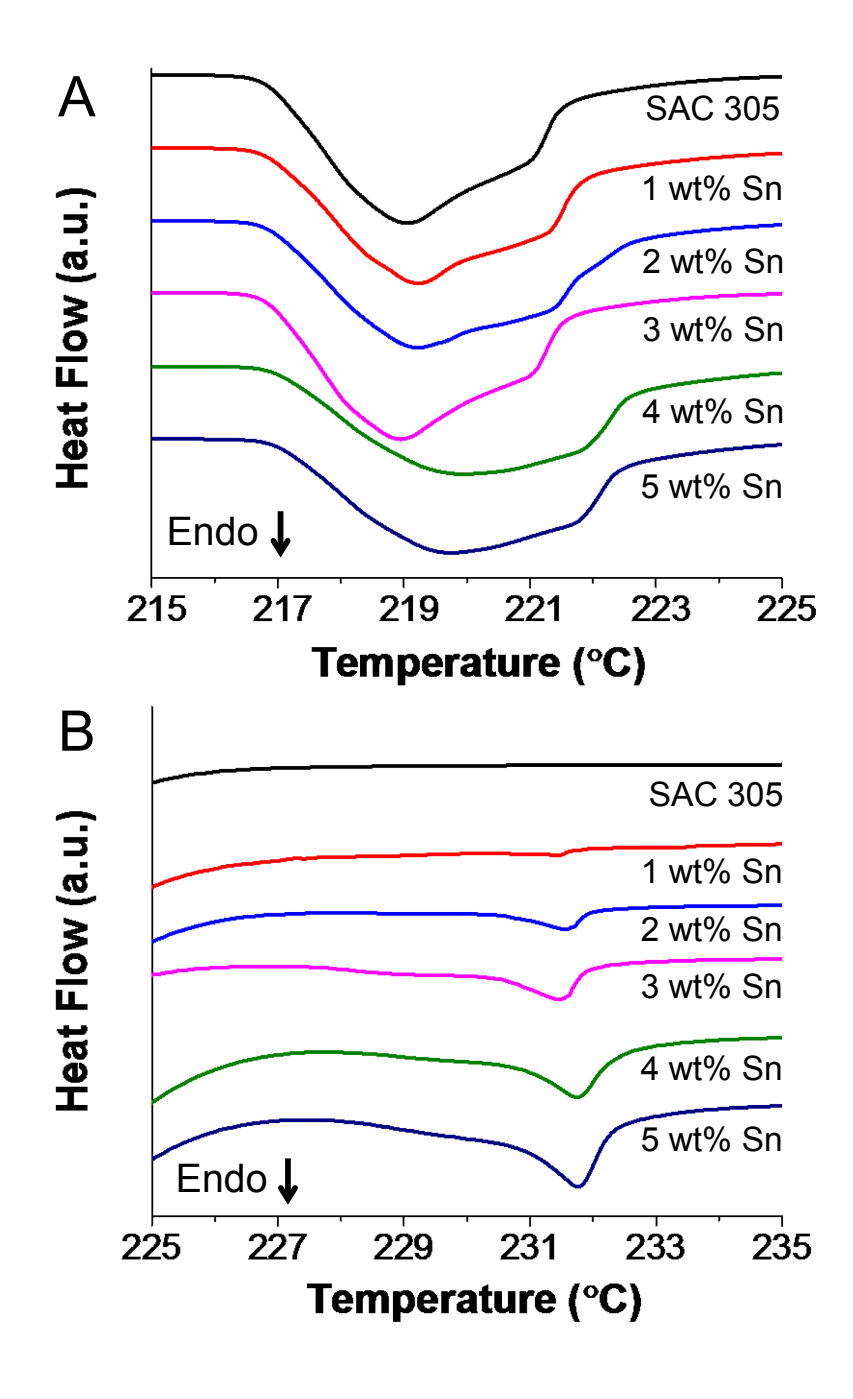


Fig. 6: DSC curves showing endothermic melting peaks for (A) SAC 305 and (B) Sn nanoparticle in the prepared nanocomposite solder pastes.

Figure 6B shows the Sn melting peaks during the initial paste heating in the temperature range from 225 °C to 235 °C, with various Sn nanoparticle additions. It was observed that the

endothermic peaks associated with Sn nanoparticle melting began to broaden and became larger as more nanoparticles were added to the paste. This was most obvious for the highest loading of Sn nanoparticles (5 wt%), where the onset of melting is 231.3 °C and the peak temperature is 232.0 °C (see Table 1).

A second heating cycle after a controlled cooling at 10 K/min was used to characterize the thermal behavior of the solder materials after paste melting and solidification. The DSC scans of the endothermic melting peak associated with the SAC microsolders are shown in Figure 7A. Little difference in both the onset and peak melting temperatures was observed between different heating cycles (see Table 1). Further examination of the endothermic peaks from the Sn nanoparticle melting in Figure 7B showed the original peak melting temperature (231.5 °C) remained relatively the same; however, a new endothermic peak on the left side of the original peak was observed around 227.2 °C (denoted as peak A, see Table 1). This was evident in all pastes containing Sn nanoparticles from 1 wt% to 5 wt%, with a more pronounced peak intensity starting from 2 wt%. There appeared to be another endothermic peak emerged around 229 °C (ranged from 228.9 to 229.2 °C, denoted as peak B in Table 1), with 1 wt% sample showing a more profound peak while the other compositions from 2 wt% to 5 wt% almost invisible. The appearance of new endothermic peaks suggested that SAC 305 micropowders and pure Sn nanoparticles in the nanocomposite solder pastes may have interacted with each other and formed new alloys. Different compositions between SAC 305 and pure Sn nanoparticles, upon heating, may have resulted in atomic interdiffusion between the two compounds and led to new alloy formation.

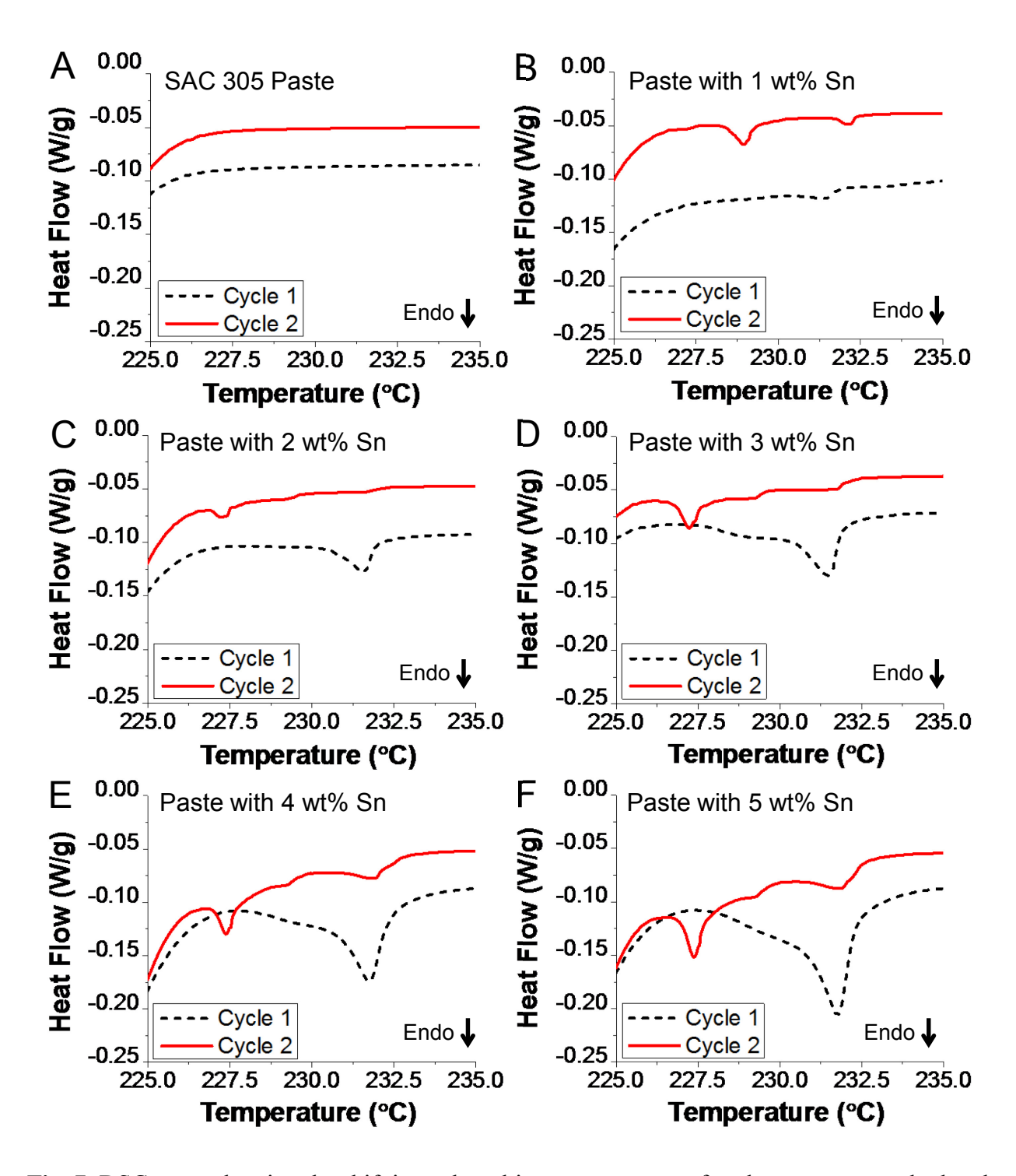


Fig. 7: DSC scans showing the shift in peak melting temperatures after the paste was melted and solidified in (A) SAC 305, (B) 1 wt% Sn, (C) 2 wt% Sn, (D) 3 wt% Sn, (E) 4 wt% Sn and (F) 5 wt% Sn prepared solder pastes.

Table 1: Summary of the onset, peak and endset of melting temperatures for nanocomposite solder pastes prepared with SAC microsolders and Sn nanoparticles.

| Sn NPs (wt%) | SAC 305 Microsolder Peaks | | | | | | Sn Nanosolder Peaks | | | | | | Peaks Emerged in Second | |
|-----------------|---------------------------|-------|--------|-----------------|-------|--------|---------------------|-------|--------|-----------------|-------|--------|-------------------------|------------|
| | Heating Cycle 1 | | | Heating Cycle 2 | | | Heating Cycle 1 | | | Heating Cycle 2 | | | Heating Cycle | |
| | Onset | Peak | Endset | | Peak | Endset | | Peak | Endset | | Peak | Endset | | New Peak B |
| | (°C) | (°C) | (°C) | (°C) | (°C) | (°C) | (°C) | (°C) | (°C) | (°C) | (°C) | (°C) | (°C) | (°C) |
| 0 | 217.2 | 219.2 | 222.8 | 217.4 | 219.4 | 222.6 | ı | - | - | - | • | - | - | - |
| 1 | 217.2 | 220.0 | 222.6 | 217.5 | 219.3 | 222.3 | 230.5 | 231.5 | 231.9 | 231.2 | 232.2 | 232.4 | 227.2 | 228.9 |
| 2 | 217.2 | 220.2 | 223 | 217.5 | 219.5 | 222.6 | 230.5 | 231.6 | 232.0 | 230.9 | 231.7 | 232.0 | 227.3 | 229.2 |
| 3 | 217.2 | 218.2 | 222.7 | 217.4 | 217.3 | 222.1 | 230.4 | 231.4 | 232.1 | 230.5 | 231.6 | 232.3 | 227.4 | 229.2 |
| 4 | 217.4 | 219.0 | 221.9 | 217.2 | 218.9 | 221.9 | 230.6 | 231.6 | 232.4 | 230.7 | 231.9 | 232.3 | 227.4 | 228.9 |
| 5 | 217.3 | 219.0 | 221.9 | 217.2 | 218.8 | 221.9 | 230.5 | 231.6 | 232.5 | 230.5 | 231.7 | 232.4 | 227.5 | 229.0 |

3.4 Enthalpy of Melting in Nanocomposite Pastes

The DSC curves were further analyzed to understand how the SAC 305 microsolders and Sn nanoparticles behaved when heated above the liquidus temperature of both materials by calculating the normalized enthalpy of melting (J/g paste). Comparing the initial heating cycle to the second heating cycle, a change in the enthalpy of melting indicated an interaction between the SAC 305 powders and Sn nanoparticles. Each endothermic peak was analyzed, with the results of each shown in Figure 8. Comparing the enthalpy of melting between cycles for the SAC micropowders in Figure 8A shows an overall decrease in the enthalpy of melting for all pastes with added Sn nanoparticles. The SAC 305 paste, containing no Sn nanoparticles as a control, showed no change in the measured enthalpy of melting. Adding Sn nanoparticles decreased the SAC enthalpy of melting in all nanocomposite solder pastes. Figure 8B shows that the enthalpy of melting associated with the Sn nanoparticles also decreased with an increase of Sn nanoparticle additions, further suggesting that the SAC 305 micropowders interacted with the pure Sn nanoparticles to form additional alloys.

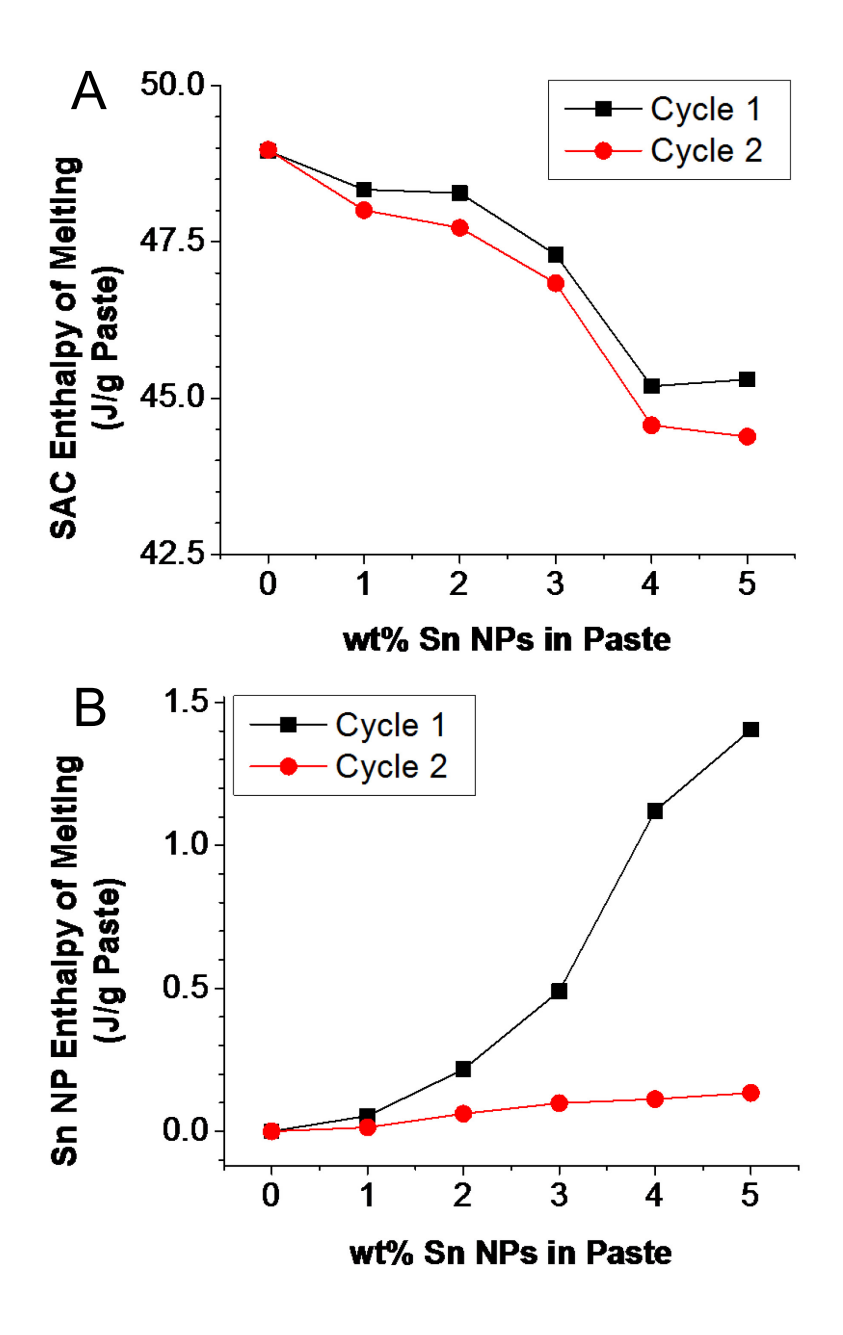


Fig. 8: Calculated enthalpies for (A) SAC melting and (B) Sn nanoparticle melting, comparing the initial melting (cycle 1) to a second heating cycle after paste melting and solidification (cycle 2).

3.5 TGA Measurements of Nanocomposite Solder Pastes

The nanocomposite solder pastes were measured by TGA to study the effects of the added Sn nanoparticles on weight loss of the solder pastes during heating, as shown in Figure 9. Figure 9A

shows the results of the TGA measurements, scanned at 10 K/min, of the prepared pastes with Sn nanoparticle additions. Significant weight loss can be observed in all pastes that can be attributed to evaporation and degradation of the flux material. The pastes, designed with 82.5 wt% total solder loading, were observed to retain over 93 % of their initial weight up to 250 °C with a maximum weight loss rate occurring around 150 °C, shown in Figure 9B. When heated to above 250 °C, two additional peaks around 360 °C and 430 °C were observed in Figure 9B, indicating flux residue decomposition was significant at these temperatures. Since the Indium 8.9E is rosinbased (ROL1) flux, it is possible that the two peaks at 360 °C and 430 °C represent boiling or decomposition from the components of the rosin. Figure 9C shows the final weight remaining after the solder pastes were measured by TGA, up to 500 °C. The paste without any added Sn nanoparticles was measured to retain approximately 85 wt% of its original mass. Adding Sn nanoparticles increased the amount of weight retained in the solder pastes, e.g., ~86.5 wt% of original mass was retained when 5 wt% Sn nanoparticles added in the paste. It is believed that the additional surface area generated by adding Sn nanoparticles helped the interactions between the micropowders, nanoparticles, and the flux, which is likely the reason for more weight remaining in the pastes.

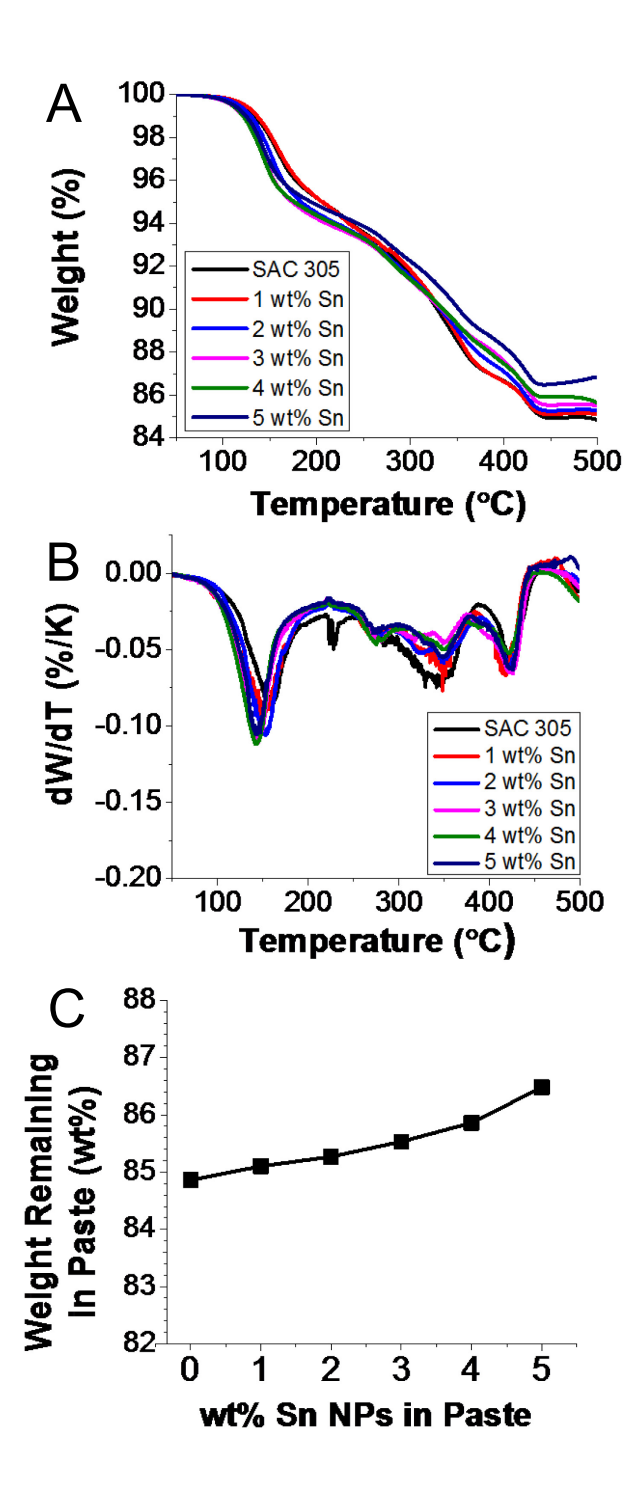


Fig. 9: TGA measurements of SAC 305 solder pastes with Sn nanoparticle additions showing (A) weight loss of nanocomposite pastes during heating, (B) derivative weight loss curves and (C) paste weight remaining after heating to 500 °C at 10 K/min in air atmosphere.

4. Conclusions

Nanocomposite solder pastes prepared with SAC 305 micropowders and Sn nanoparticles were investigated for their thermal properties by DSC and TGA. DSC measurements of the nanocomposite pastes exhibited new endothermic peaks, in addition to the two original peaks from the SAC microsolders and Sn nanoparticles, suggesting that the SAC 305 microsolder powders and pure Sn nanoparticles interacted during the heating process to form additional alloys. Changes in the enthalpy of melting associated with each material further suggested the interactions between the SAC microsolders and Sn nanoparticles during the paste heating. TGA measurements also indicated that adding Sn nanoparticles to the SAC pastes increased the interaction between the SAC microsolders and Sn nanoparticles, and the nanocomposite pastes retained more weight from their original paste than the SAC paste alone.

Acknowledgements

This research was supported by the National Science Foundation (Award # IIP-1640643). The authors would like to thank Indium Corporation of America (Clinton, NY) for providing micropowders and paste flux materials used in this research.

Declaration of interest

The authors declare that they have no known competing financial interests or personal relationships that could have appeared to influence the work reported in this paper.

References

- 1. Abtew, M. and G. Selvaduray, *Lead-free Solders in Microelectronics*. Materials Science and Engineering: R: Reports, 2000. **27**(5–6): p. 95-141.
- 2. Kang, S.K. and A.K. Sarkhel, *Lead (Pb)-free solders for electronic packaging*. Journal of Electronic Materials, 1994. **23**(8): p. 701-707.
- 3. Glazer, J., *Metallurgy of low temperature Pb-free solders for electronic assembly.* International Materials Reviews, 1995. **40**(2): p. 65-93.
- 4. Manko, H.H., *Soldering handbook for printed circuits and surface mounting*. 1995: Springer Science & Business Media.
- 5. Bukat, K., et al., Silver nanoparticles effect on the wettability of Sn-Ag-Cu solder pastes and solder joints microstructure on copper. Soldering & Surface Mount Technology, 2011. **23**(3): p. 150-160.
- 6. Date, M., et al. *Impact reliability of solder joints*. in *Electronic Components and Technology Conference*, 2004. Proceedings. 54th. 2004. IEEE.
- 7. Ho, C., et al., Effect of Cu concentration on the reactions between Sn-Ag-Cu solders and Ni. Journal of Electronic Materials, 2002. **31**(6): p. 584-590.
- 8. Liu, P.L., Z. Xu, and J.K. Shang, *Thermal stability of electroless-nickel/solder interface: Part A. Interfacial chemistry and microstructure.* Metallurgical and Materials Transactions A, 2000. **31**(11): p. 2857-2866.
- 9. Nishiura, M., et al., *Mechanical strength and microstructure of BGA joints using lead-free solders*. Materials Transactions, 2002. **43**(8): p. 1802-1807.
- 10. Shohji, I., et al., *Interface reaction and mechanical properties of lead-free Sn-Zn alloy/Cu joints*. Materials Transactions, 2002. **43**(8): p. 1797-1801.
- 11. Suganuma, K., et al., *Heat resistance of Sn–9Zn solder/Cu interface with or without coating.* Journal of Materials Research, 2000. **15**(4): p. 884-891.
- 12. Tu, K.-N. and K. Zeng, *Tin–lead (SnPb) solder reaction in flip chip technology*. Materials science and engineering: R: reports, 2001. **34**(1): p. 1-58.
- 13. Zeng, K. and K.-N. Tu, Six cases of reliability study of Pb-free solder joints in electronic packaging technology. Materials Science and Engineering: R: reports, 2002. **38**(2): p. 55-105.
- 14. Chang, S.-Y., Y.-C. Huang, and Y.-M. Lin, *Mechanical property and fracture behavior characterizations of 96.5 Sn-3.0 Ag-0.5 Cu solder joints*. Journal of Alloys Compounds, 2010. **490**(1-2): p. 508-514.

- 15. McCormack, M., et al., *New Pb*Applied Physics Letters, 1993. **63**(1): p. 15-17.
- Wade, N., et al., Effects of Cu, Ag and Sb on the creep-rupture strength of lead-free solder alloys. Journal of Electronic Materials, 2001. **30**(9): p. 1228-1231.
- 17. Anderson, I.E., et al., *Alloying effects in near-eutectic Sn-Ag-Cu solder alloys for improved microstructural stability*. Journal of Electronic Materials, 2001. **30**(9): p. 1050-1059.
- 18. Miller, C.M., I.E. Anderson, and J.F. Smith, *A viable tin-lead solder substitute: Sn-Ag-Cu*. Journal of Electronic Materials, 1994. **23**(7): p. 595-601.
- 19. Loomans, M.E., M.E.J.M. Fine, and M.T. A, *Tin-silver-copper eutectic temperature and composition*. 2000. **31**(4): p. 1155-1162.
- 20. Moon, K.-W., et al., *Experimental and thermodynamic assessment of Sn-Ag-Cu solder alloys.* 2000. **29**(10): p. 1122-1136.
- Wu, C.M.L., et al., *Microstructure and mechanical properties of new lead-free Sn-Cu-RE solder alloys.* Journal of Electronic Materials, 2002. **31**(9): p. 928-932.
- 22. Amagai, M., *A study of nanoparticles in Sn–Ag based lead free solders*. Microelectronics Reliability, 2008. **48**(1): p. 1-16.
- Guo, F., J. Lucas, and K. Subramanian, *Creep behavior in Cu and Ag particle-reinforced composite and eutectic Sn-3.5 Ag and Sn-4.0 Ag-0.5 Cu non-composite solder joints*. Journal of Materials Science: Materials in Electronics, 2001. **12**(1): p. 27-35.
- 24. Liu, J., et al., *Development of creep-resistant, nanosized Ag particle-reinforced Sn-Pb composite solders.* Journal of Electronic Materials, 2004. **33**(9): p. 958-963.
- 25. Lin, D., et al., An investigation of nanoparticles addition on solidification kinetics and microstructure development of tin–lead solder. Materials Science and Engineering: A, 2003. **360**(1-2): p. 285-292.
- 26. Tsao, L., et al., *Influence of TiO2 nanoparticles addition on the microstructural and mechanical properties of Sn0. 7Cu nano-composite solder.* Materials Science and Engineering: A, 2012. **545**: p. 194-200.
- Wu, J., et al., Effects of α-Al 2 O 3 nanoparticles-doped on microstructure and properties of Sn-0.3 Ag-0.7 Cu low-Ag solder. Journal of Materials Science: Materials in Electronics, 2018. **29**(9): p. 7372-7387.
- 28. Kao, S.-T., Y.-C. Lin, and J.-G. Duh, *Controlling intermetallic compound growth in SnAgCu/Ni-P solder joints by nanosized Cu6Sn5 addition*. Journal of Electronic Materials, 2006. **35**(3): p. 486-493.

- 29. Nai, S., J. Wei, and M. Gupta, *Interfacial intermetallic growth and shear strength of lead-free composite solder joints*. Journal of Alloys and Compounds, 2009. **473**(1-2): p. 100-106.
- 30. Chen, S., et al., *A reliability study of nanoparticles reinforced composite lead-free solder.* Materials Transactions, 2010. **51**(10): p. 1720-1726.
- 31. Lin, D., et al., *Understanding the influence of copper nanoparticles on thermal characteristics and microstructural development of a tin-silver solder*. Journal of Materials Engineering and Performance, 2007. **16**(5): p. 647-654.
- 32. Jiang, H., et al., *Size-dependent melting properties of tin nanoparticles*. Chemical Physics Letters, 2006. **429**(4): p. 492-496.
- 33. Koppes, J.P., et al., *Utilizing the thermodynamic nanoparticle size effects for low temperature Pb-free solder*. Materials Science and Engineering: B, 2012. **177**(2): p. 197-204.
- 34. Jiang, H., Synthesis of tin, silver and their alloy nanoparticles for lead-free interconnect applications. 2008.
- 35. Jiang, H., et al., *Synthesis and thermal and wetting properties of tin/silver alloy nanoparticles for low melting point lead-free solders*. Chemistry of Materials, 2007. **19**(18): p. 4482-4485.
- 36. Jiang, H., K.-s. Moon, and C. Wong, *Tin/silver/copper alloy nanoparticle pastes for low temperature lead-free interconnect applications*, in *Electronic Components and Technology Conference*, 2008. ECTC 2008. 58th. 2008, IEEE. p. 1400-1404.
- 37. Liu, J., et al. Recent development of nano-solder paste for electronics interconnect applications. in Electronics Packaging Technology Conference, 2008. EPTC 2008. 10th. 2008. IEEE.
- 38. Std, I., *J-STD-005*, in *Requirements for Soldering Pastes*. 1995.
- 39. Kotadia, H.R., P.D. Howes, and S.H. Mannan, *A review: On the development of low melting temperature Pb-free solders*. Microelectronics Reliability, 2014. **54**(6): p. 1253-1273.
- 40. Huang, B., A. Dasgupta, and N.-C. Lee, *Effect of SnAgCu composition on soldering performance*. Journal of Soldering Surface Mount Technology, 2005. **17**(3): p. 9-19.
- 41. American Institute of Physics Handbook. 3rd ed. 1972, New York: McGraw-Hill. 4 243.

Graphical Abstract

